

Preparation of Magnesium-Doped Hydroxyapatite Coating on the Surface of Carbon/Carbon Composites [Postprint]

Authors: Ni Xinye, Li Aijun, Bai Ruicheng, Xiong Xinbai, Zhou Dong

Date: 2023-03-18T00:00:00+00:00

Abstract

Hydroxyapatite coatings with magnesium content equivalent to that of human bone were prepared on carbon/carbon composite surfaces via electromagnetic induction, with magnesium weight percentages in the coatings of 0, 0.28%, 0.32%, and 0.49%, respectively. The coatings were characterized by SEM, EDS, XRD, FT-IR, and other techniques. The results indicate that magnesium ions can incorporate into the hydroxyapatite crystal lattice, and coatings with different magnesium contents exhibit slight differences in phase composition. Within the range of magnesium content in human bone, higher magnesium content in the coatings enhances the adhesion, proliferation, and differentiation abilities of in vitro rat osteoblasts (MC3T3-E1).

Full Text

Preparation of Magnesium-Doped Hydroxyapatite Coating on Carbon/Carbon Composites

NI Xinye^{1,2,3}, LI Aijun¹, BAI Ruicheng¹, XIONG Xinbo³, ZHOU Dong²

¹College of Materials Science and Engineering, Shanghai University, Shanghai 200072, China

²Changzhou Institute of Technology, Changzhou 213002, China

³College of Materials Science and Engineering, Shenzhen University, Shenzhen 518060, China

Supported by Postdoctoral Science Foundation of China No. 2014M560323, the municipal social development project of Changzhou City No. CJ20130019, and Natural Science Foundation of Jiangsu Province No. BK20151181.

Manuscript received January 14, 2015; in revised form March 25, 2015

To whom correspondence should be addressed, Tel: (0519)88118730,
E-mail: nxy2000@aliyun.com

Abstract

Mg-doped hydroxyapatite coatings with magnesium weight percentages of 0, 0.28%, 0.32%, and 0.49%, comparable to human bone composition, were prepared on carbon/carbon composites using electromagnetic induction method. The coatings were characterized by SEM, EDS, XRD, and FT-IR. Results demonstrated that Mg^{2+} ions could enter the hydroxyapatite crystal lattice, with only minor phase differences observed among coatings with varying Mg content. Within the physiological Mg content range of human bone, higher Mg content in the coatings significantly enhanced the adhesion, proliferation, and differentiation capacity of rat osteoblasts (MC3T3-E1) *in vitro*.

KEY WORDS composites, carbon/carbon composites, magnesium, hydroxyapatite

Carbon is an essential element in the human body [1]. Carbon/carbon (C/C) composites offer numerous advantages including high strength, high toughness, corrosion resistance, high temperature tolerance, and an elastic modulus comparable to human bone [2]. Medical-grade C/C composites represent a novel biomedical material reinforced with carbon fibers in a carbon matrix, showing promising potential for artificial joint and bone prosthesis applications [3]. However, untreated C/C composite surfaces are hydrophobic and biologically inert [4], forming only mechanical bonds with bone tissue without the capacity to conduct or induce bone regeneration. Additionally, the interfacial formation period is prolonged, preventing chemical bonding with the host tissue [5], which extends implant fixation time and limits clinical application [6]. Furthermore, C/C composite particles are prone to detachment [4], necessitating surface modification [7].

Hydroxyapatite (HA, chemical formula $Ca_{10}(PO_4)_6(OH)_2$) occurs naturally in animal bone and tooth tissues as a bioactive material. While HA exhibits strong bonding with bone, its insufficient strength and toughness preclude its use as a standalone bone replacement material. Combining the advantages of C/C composites and HA can satisfy clinical requirements for bone substitute materials, specifically using C/C composites as substrates with HA surface coatings [8,9]. Pure HA is susceptible to dissolution in physiological environments, leading to instability and implant failure [10], and its bioactivity is inferior to natural bone mineral [11]. Natural bone contains not only apatite but also Mg^{2+} , Na^+ , F^- , and other ions. Mg^{2+} concentration directly influences bone calcification processes, decreasing from the initiation to completion of calcification. Magnesium

constitutes 0.26%-0.55% by weight in natural bone, with adult humans containing approximately 1000 mmol (24 g) of Mg, of which about 60% resides in bone, 39% intracellularly, and only 1% in the extracellular environment [12].

Jasminka et al. [13] found that Mg regulates bone growth and remodeling by participating in bone mineral surface reactions. Magnesium is involved in normal cell proliferation and stimulates DNA and protein synthesis [14]. Yamazaki et al. demonstrated at the molecular level that Mg incorporation into apatite crystals accelerates osteoblast adhesion and promotes bone formation [15]. Mg-HA containing 2 mol% Mg significantly enhances osteoblast attachment compared to pure HA [16]. However, Serre et al. showed that adding 20% Mg reduces bone conductivity, indicating that excessive functional element doping can compromise biological functionality [17]. Thus, appropriately Mg-doped HA coatings represent clinically significant modified materials, with Mg-HA composites overcoming the lack of osteoinductive capacity in conventional bioceramics [18].

Current research focuses on Mg-doped HA preparation [19-21] and coating deposition on metal substrates using sol-gel, electrochemical, and plasma spraying methods [22,23,9]. However, these techniques cannot adequately address the weak bonding strength between pure HA coatings and C/C composites [9,24,25]. Moreover, Mg²⁺ incorporation causes lattice distortion, making coating preparation more challenging than pure HA. The authors previously prepared monetite and HA coatings on C/C composites via electromagnetic induction (15 kHz), achieving a scratch test critical load of 18 N [26], meeting clinical requirements. This study employs electromagnetic induction to prepare Mg-doped HA coatings on C/C composites with Mg content comparable to human bone.

1.1 Preparation of Carbon/Carbon Composites

The experimental C/C composites were 2.5-dimensional PAN-based materials with a bending strength of 182.3 MPa, bending modulus of 90.4 GPa, and elastic modulus of 35.0 GPa, machined into cylinders (diameter 1.2 cm, height 0.6 cm). To enhance coating-substrate adhesion, C/C specimens were placed in an autoclave with 40 mL of 2 M H₂O₂ [26] at 150°C. The electromagnetic induction heating frequency was adjusted to 15 kHz. Ca(NO₃)₂, Mg(NO₃)₂, and NH₄H₂PO₄ were dissolved in distilled water with Ca and P ion concentrations of 0.080 and 0.048 mol/L, respectively, and Mg ion concentrations of 0, 0.04, 0.08, and 0.16 mol/L, designated as Mg0M, Mg0.04M, Mg0.08M, and Mg0.16M. The pH was adjusted to 4.5.

Deposition was performed at room temperature (20°C) with a current of 650 A for 2 h. After deposition, samples were rinsed with distilled water to obtain Mg-doped calcium phosphate coatings. Samples were then immersed in a solution at 130°C to convert the coatings to Mg-doped HA. Finally, coatings were soaked and rinsed with deionized water, then heated at 180°C for 0.5 h to remove residual water.

1.2 Material Characterization

HA coatings were characterized by X-ray diffraction (XRD), scanning electron microscopy (SEM), and Fourier-transform infrared spectroscopy (FT-IR). XRD was performed using a D8 diffractometer (40 kV, 40 mA, step size 0.01° , scan range 10° - 90°). SEM and EDS were conducted using a SUPRA55 microscope at 15 kV acceleration voltage. FT-IR analysis employed a NEXU670 spectrometer.

1.3 Rat Osteoblast (MC3T3-E1) Adhesion and Proliferation

Coated samples were placed in 24-well plates, each receiving 1 mL of culture medium containing 2×10^4 MC3T3-E1 cells/mL. The medium consisted of RPMI1640 and DMEM supplemented with 10% fetal bovine serum, 100 g/mL streptomycin, and 100 units/mL penicillin. Cells were incubated at 37°C with 5% CO_2 to allow natural sedimentation onto coating surfaces. After 5 h, the medium was aspirated, samples were washed with PBS, and transferred to new 24-well plates with fresh medium.

Experimental procedures included: (1) After 24 h, samples were washed with PBS, fixed with 2.5% glutaraldehyde for 2 h, dehydrated sequentially with 30%, 50%, 70%, 90%, and 95% ethanol (20 min each), then exchanged with isoamyl acetate for SEM observation of cell adhesion. (2) After 2 days, proliferation was assessed by fluorescence microscopy. Samples were washed with PBS, fixed with 10% formaldehyde at room temperature for 15 min, stained with 5 g/mL propidium iodide (PI, Sigma) for 15 min, mounted with anti-fade solution, and examined using an OLYMPUS IX71 inverted fluorescence microscope. (3) Cell proliferation was quantified at three time points (2, 4, and 6 days) with five replicate samples per group. Cells were detached with trypsin, resuspended in PBS, and counted using a hemocytometer. Total cell numbers per sample were calculated and averaged. Statistical analysis was performed using one-way ANOVA with SPSS 11.0 software.

2.1 Coating Morphology (SEM and EDS)

[Figure 1: see original paper] shows SEM images of pure HA (Mg0M) and Mg-doped coatings. The pure HA coating consisted of rod-like crystals approximately 500 nm long and 50 nm in diameter, clustered in bundles of ten or more rods with visible interstitial spaces. The Mg0.04M coating comprised rods about 350 nm long and 50 nm in diameter, forming bundles of 5-10 rods. The Mg0.08M coating featured rod-like crystals approximately 400 nm long with inter-bundle spaces of 150-400 nm; bundle structures increased, exhibiting “tapered tip-thick root” morphology with gradually decreasing interstitial spaces. The Mg0.16M coating formed a dense structure of cylindrical rod-like crystals. Researchers suggest that appropriately sized micropores facilitate cell adhesion and metabolic exchange [27].

EDS analysis of Mg0.04M, Mg0.08M, and Mg0.16M coatings [Figure 0: see original paper] revealed Mg weight percentages of 0.28%, 0.32%, and 0.49%,

respectively, comparable to human bone Mg content. The Mg0M coating was pure HA (0% Mg).

2.2 XRD Analysis

[Figure 3: see original paper] presents XRD patterns of pure and Mg-doped HA, showing formation of Mg-substituted HA with small crystallite sizes [Figure 2: see original paper]. Mg incorporation caused convergence of major XRD peaks at 28.032° (102) and 28.841° (210), with peak separation decreasing by 0.14° between Mg0.08M and Mg0M. Similarly, peaks at 32.117° (112) and 32.814° (300) converged, with separation reduced by 0.12° between Mg0.08M and Mg0M. This results from Mg^{2+} (ionic radius 0.078 nm) substituting for Ca^{2+} (0.106 nm), decreasing interplanar spacing.

2.3 FTIR Analysis

FTIR spectra of Mg-doped HA coatings are shown in [Figure 4: see original paper]b-d. Phosphate group stretching vibrations appear at 1091 cm^{-1} , 1034 cm^{-1} , and 965 cm^{-1} , with bending vibrations at 603 cm^{-1} , 566 cm^{-1} , and 481 cm^{-1} . Hydroxyl group absorptions occur at 1654 cm^{-1} and 3447 cm^{-1} [28,29], while the characteristic HA peak at 638 cm^{-1} is present; the 3582 cm^{-1} HA peak may be obscured by hydroxyl absorption [30]. These results indicate that Mg incorporation does not fundamentally alter coating composition compared to pure HA [Figure 4: see original paper]a.

2.4 Cell Adhesion

MC3T3-E1 cell morphology after 24 h on different coatings is shown in [Figure 5: see original paper]. On Mg0M coatings, cells remained spherical with poor attachment. On Mg0.04M coatings, cells showed slight spreading. On Mg0.08M coatings, cells adhered tightly to the surface. On Mg0.16M coatings, cells fully spread with pseudopodia extending along the coating surface. Cell adhesion behavior is influenced by the microenvironment. Mg doping of HA surfaces creates conditions more similar to natural bone, promoting cell adhesion. Cell spreading increases surface area, enhancing contact with culture medium and facilitating nutrient uptake, thereby promoting growth and proliferation. Researchers have confirmed that low-concentration Mg doping (<5%) improves biological performance [33,34]. Enhanced osteoblast proliferation on Mg-doped HA coatings likely relates to the presence of physiologically relevant Mg^{2+} concentrations similar to natural bone.

2.5 Cell Proliferation

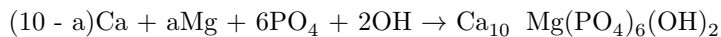
[Figure 6: see original paper] shows proliferation curves of MC3T3-E1 cells cultured for 2, 4, and 6 days. Mg-doped HA coatings exhibited significantly higher cell proliferation than pure HA coatings. Statistical

analysis using one-way ANOVA (SPSS 11.0) revealed significant differences: at 2 days, P values were 4.9×10^{-5} , 2.0×10^{-6} , and 2.2×10^{-6} for Mg0.04M, Mg0.08M, and Mg0.16M versus Mg0M, respectively; at 4 days, P values were 1.2×10^{-5} , 1.0×10^{-6} , and 8.1×10^{-7} ; at 6 days, P values were 2.0×10^{-4} , 6.6×10^{-5} , and 7.9×10^{-6} (all $< 5.0 \times 10^{-2}$), indicating statistically significant differences in proliferation.

2.6 Fluorescence Microscopy of Cell Proliferation

Fluorescence microscopy revealed significantly fewer MC3T3-E1 cells on pure HA (Mg0M) coatings compared to Mg0.04M, Mg0.08M, and Mg0.16M coatings, with the highest cell densities observed on Mg0.08M and Mg0.16M coatings. These observations [Figure 7: see original paper] correlate with cell counting results.

Based on electromagnetic induction principles, when alternating current passes through the coil, the C/C composite substrate generates an induced electromotive potential, creating eddy currents that produce Joule heating. The resulting temperature increase heats the surrounding solution. The chemical reaction equation is:



Mg²⁺ substitution for Ca²⁺ causes HA crystal structure distortion and reduced crystallinity, limiting the extent of substitution. Mg²⁺ replaces Ca(I) and Ca(II) sites, preferentially substituting Ca(II) positions along the OH channel [31]. Bigi et al. proposed that Mg preferentially substitutes Ca atoms adjacent to hydroxyl groups due to oxygen proximity [32]. Studies have confirmed that low-concentration Mg-doped HA coatings (<5% Mg) enhance biological effects [33,34]. The accelerated osteoblast proliferation on Mg-doped HA coatings likely relates to the presence of physiologically relevant Mg²⁺ concentrations matching natural bone composition.

3 Conclusion

Mg-doped hydroxyapatite coatings prepared by electromagnetic induction exhibit Mg content comparable to human bone. These coatings show minor phase differences from pure HA coatings. Within the physiological Mg content range of human bone, higher coating Mg content significantly enhances osteoblast adhesion, proliferation, and differentiation *in vitro*.

References

1. Gott VL, Whiffen JD, Dutten RC. Heparin bonding colloidal graphite surfaces. *Science*. 1963;142(3597):1279.
2. NI Xinye, TANG Xiaobin, GENG Changran, CHEN Da. The prospect of carbon fiber implants in radiotherapy. *J Appl Clin Med Phys*. 2012;13(4):152.

3. Meier R, Schulz M, Krimmer H, Stütz N, Lanz U. Proximal interphalangeal joint replacement with pyrolytic carbon prostheses. *Oper Orthopade Traum.* 2007;19(1):1.
4. Shimmin A, Beaulé PE, Campbell P. Metal-on-metal hip resurfacing arthroplasty. *J Bone Joint Surg Am.* 2008;90(3):637.
5. Adams D, Williams DF. The response of bone to carbon-carbon composites. *Biomaterials.* 1984;5(2):59.
6. Gwyn MJ, Francisco XC. Biomedical applications of carbon fiber reinforced carbon in implanted prostheses. *Carbon.* 1977;15(1):33.
7. NI Xinye, LI Aijun, XIONG Xinbo, BAI RuiCheng, ZHOU Dong. Effect electromagnetic induction deposition' s heating time of magnesium-hydroxyapatite coating on carbon/carbon composites. *Journal of Biobased Materials and Bioenergy.* 2014;8(6):603.
8. NI Xinye, CHU Cencen, XIONG Xinbo, LI Aijun, BAI Ruicheng. Preparation of hydroxyapatite coating using chemical liquid vaporization deposition on carbon/carbon composites. *RSC Advances.* 2014;4(77):41129.
9. NI Xinye, TANG Xiaobin, LIN Tao, ZHAO Quandi, GENG Changran, CAI Leiming, GU Weidong, MIAO YunLiang, CHEN Da. Properties of plasma-spray coated hydroxyapatite on carbon/carbon composites pretreated by an argon plasma. *New Carbon Material.* 2013;28(3):215.
10. Sui J, Li M, Lu Y, Yin L, Song Y. Plasma-sprayed hydroxyapatite coatings on carbon/carbon composites. *Surface and Coatings Technology.* 2004;176(2):188.
11. Kalita SJ, Bhatt HA. Nanocrystalline hydroxyapatite doped with magnesium and zinc: synthesis and characterization. *Mater Sci Eng C.* 2007;27(4):837.
12. Wester P. Magnesium. *Am J Clin Nutr.* 1987;45:1305.
13. Ilich JZ, Kerstetter JE. Nutrition in bone health revisited: a story beyond calcium. *J Am Coll Nutr.* 2000;19(6):715.
14. Wolf FI, Cittadini A. Magnesium in cell proliferation and differentiation. *Front Biosci.* 1999;4:607.
15. Yamazaki Y, Uchida T. Action of FGMgCO₃Ap-collagen composite in promoting bone formation. *Biomaterials.* 2003;24(27):4913.
16. Webster TJ, Ergun C, Doremus RH, Bizios R. Hydroxylapatite with substituted magnesium, zinc, cadmium, and yttrium. II. Mechanisms of osteoblast adhesion. *J Biomed Mater Res.* 2002;59(2):2002.
17. Serre CM, Papillard M, Chavassieux P, Voegel JC, Boivin G. Influence of magnesium substitution on a collagen-apatite biomaterial on the production of a calcifying matrix by human osteoblasts. *J Biomed Mater Res.* 1998;42(4):626.
18. Pijocha D, Zima A, Paszkiewicz Z, Ślósarczyk A. Physicochemical properties of the novel biphasic hydroxyapatite-magnesium phosphate biomaterial. *Acta Bioeng Biomech.* 2013;15(3):53.
19. Zyman Z, Tkachenko M, Epple M, Polyakov M, Naboka M. Magnesium-substituted hydroxyapatite ceramics. *Materialwissenschaft und Werkstofftechnik.* 2006;37(6):474.

20. Ziani S, Meski S, Khireddine H. Characterization of magnesium-doped hydroxyapatite prepared by sol-gel process. *International Journal of Applied Ceramic Technology*. 2014;11(1):83.
21. Cai Y, Zhang S, Zeng X, Wang Y, Qian M, Weng W. Improvement of bioactivity with magnesium and fluorine ions incorporated hydroxyapatite coatings via sol-gel deposition on Ti6Al4V alloys. *Thin Solid Films*. 2009;517(17):5347.
22. Jiao M, Wang X. Electrolytic deposition of magnesium-substituted hydroxyapatite crystals on titanium substrate. *Materials Letters*. 2009;63(27):2286.
23. Wang C, Li K, Zhai Y, Li H, Wang J, Jiao G. Study of fluor-hydroxyapatite coatings on carbon/carbon composites. *Surface and Coatings Technology*. 2009;203(13):1771.
24. Xiong X, Ni X, Zeng X, Ji Z. A study of monetite precipitation on HT-C/C composites by induction heating method at different substrate temperatures. *Surface and Coatings Technology*. 2013;256(5):6.
25. Hench LL. Sol-gel materials for bioceramic applications. *Curr Opin Solid State Mater Sci*. 1997;2(5):604.
26. Gomes S, Renaudin G, Jallot E, Nedelec JM. Structural characterization and biological fluid interaction of sol-gel-derived Mg-substituted biphasic calcium phosphate ceramics. *ACS Appl Mater Interfaces*. 2009;1(2):505.
27. Landi E, Logroscino G, Proietti L, Tampieri A, Sandri M, Sprio S. Biomimetic Mg-substituted hydroxyapatite: from synthesis to *in vivo* behaviour. *J Mater Sci Mater Med*. 2008;19(1):239.
28. Laurencin D, Almora-Barrios N, de Leeuw NH, Gervais C, Bonhomme C, Mauri F, Chrzanowski W, Knowles JC, Newport RJ, Wong A, Gan Z, Smith ME. Magnesium incorporation into hydroxyapatite. *Biomaterials*. 2011;32(7):1826.
29. Bigi A, Falini G, Foresti E, Gazzano M, Ripamonti A, Roveri N. Magnesium influence on hydroxyapatite crystallization. *J Inorg Biochem*. 1993;49(1):69.
30. Wang X, Zhuang J, Peng Q, Li Y. Surfactant-assisted synthesis of hydroxyapatite particles. *Materials Letters*. 2006;60(27):3227.
31. Li Y, Tjong SC. Low-temperature synthesis of hydroxyapatite at physiological temperature. *Materials Letters*. 2003;57(13-14):2066.
32. Webster TJ, Ergun C, Doremus RH, Bizios R. Hydroxylapatite with substituted magnesium, zinc, cadmium, and yttrium. II. Mechanisms of osteoblast adhesion. *J Biomed Mater Res*. 2002;59(2):2002.
33. Landi E, Logroscino G, Proietti L, Tampieri A, Sandri M, Sprio S. Biomimetic Mg-substituted hydroxyapatite: from synthesis to *in vivo* behaviour. *J Mater Sci Mater Med*. 2008;19(1):239.
34. Gomes S, Renaudin G, Jallot E, Nedelec JM. Structural characterization and biological fluid interaction of sol-gel-derived Mg-substituted biphasic calcium phosphate ceramics. *ACS Appl Mater Interfaces*. 2009;1(2):505.

Note: Figure translations are in progress. See original paper for figures.

Source: ChinaXiv – Machine translation. Verify with original.